Research Article | Vol. 29, No. 11 / 24 May 2021 / Optics Express 17613

Optics EXPRESS

Nonlinear-dissipation-induced nonreciprocal exceptional points

TAO LI,[1] ZIKAI GAO,[1] AND KEYU XIA[2,3,*]

[1]School of Science, Nanjing University of Science and Technology, Nanjing 210094, China
[2]College of Engineering and Applied Sciences, and School of Physics, Nanjing University, Nanjing 210093, China
[3]National Laboratory of Solid State Microstructures, Collaborative Innovation Center of Advanced Microstructures, Nanjing University, Nanjing 210093, China
[*]keyu.xia@nju.edu.cn

Abstract: Exceptional points (EPs) have revealed a lot of fundamental physics and promise many important applications. The effect of system nonlinearity on the property of EPs is yet to be well studied. Here, we propose an optical system with nonlinear dissipation to achieve a nonreciprocal EP. Our system consists of a linear whispering-gallery-mode microresonator (WGMR) coupling to a WGMR with nonlinear dissipation. In our system, the condition of EP appearance is dependent on the field intensity in the nonlinear WGMR. Due to the chirality of intracavity field intensity, the EPs and the transmission of the system can be nonreciprocal. Our work may pave the way to exploit nonreciprocal EP for optical information processing.

1. Introduction

Dissipation is a natural phenomenon that deviates practical quantum systems from canonical quantum mechanics described by Hermitian Hamiltonians [1,2]. Quantum systems have finite decay times and thus their evolutions are always non-unitary. In this circumstance, a quantum system can be effectively described by a non-Hermitian Hamiltonian with complex eigenvalues and nonorthogonal eigenstates [3,4]. In such a non-Hermitian system, exceptional point (EP) emerges when the coupling strength between two linear modes with the same energy goes beyond half of the dissipation difference [5–13]. Specifically, the complex eigenvalues and corresponding eigenstates simultaneously coalesce at EPs. Meanwhile, some counter-intuitive features associated with EPs enable a wide range of exciting applications, such as EP-based sensing and measurement [14–18], phonon laser [19], unidirectional invisibility [20–22], and breakdown of adiabaticity [23–25].

Whispering-gallery-mode microresonators (WGMRs) with high quality factors and microscale mode volumes can possess a high intracavity field intensity and a long photon lifetime. Thus, WGMRs provide versatile platforms for fundamental physics studies and practical applications, such as parity-time (PT) symmetry [26], optothermal dynamics [27], unidirectional laser emission [28] and quantum information processing [29]). In 2011, Wiersig predicted that the existence of two or more nanoparticles in the evanescent field of a single WGMR can lead to the appearance of EPs [30], breaking the symmetry of backscattering between two counter-propagating modes [31,32]. In 2014, Peng et al. [33] and Chang et al. [34] experimentally realized a non-Hermitian Hamiltonian and the PT-symmetry in an optical system consisting of two coupled WGMRs with gain and loss, respectively. Going further, these two groups experimentally demonstrated the PT-assisted optical nonreciprocity. Loss-induced suppression and revival of lasing have been observed by Peng et al. using two passively coupled WGMRs [35], and been theoretically discussed in detail by Shu et al. [36]. In this experiment, the pattern of the field intensities in two coupled WGMRs changes from symmetric to extremely asymmetric, namely strongly chiral, when the system transits from the strong-coupling regime to the weak-coupling one [35].

#426474 https://doi.org/10.1364/OE.426474
Journal © 2021 Received 29 Mar 2021; revised 7 May 2021; accepted 16 May 2021; published 21 May 2021

Optics EXPRESS

Furthermore, anti-PT symmetry can be realized in three passively coupled WGMRs [37] or a single microcavity [38]. In principle, EPs in WGMRs are very sensitive to the variation of system parameters. They have been exploited to control light flow in a non-reciprocal way [39–43], to enhance sensing [44–56], and to manipulate the modal content of multimode lasers [57–65].

The effect of nonlinearity on systems with PT symmetry also attacks a lot of attention. In 2013, Lumer et al. showed that Kerr nonlinearity can transform a system from broken to full PT symmetry [66]. In 2015, Hassan et al. studied the nonlinear reversal of the PT-symmetric phase transition in two coupled WGMRs with gain and loss by tuning the probe intensity [67]. Subsequently, nonlinearity-induced PT-symmetry was shown in coupled nonlinear waveguides without material gain [68] and higher-order EP in nondissipative non-Hermitian systems with parametric amplification was proposed for sensing [69,70]. Recently, nonreciprocal PT symmetry induced by stimulated Brillouin scattering was realized in two coupled WGMRs [71].

Here we propose an optical system with nonlinear dissipation to obtain nonreciprocal EPs. This system includes two passively coupled WGMRs and two side-coupling waveguides. One WGMR possesses nonlinear dissipation due to two-photon absorption [72–74]. The other is a linear WGMR. Our nonlinear dissipative system shows nonreciprocal EPs and the dependence of the EP number on the input field, which are significantly different from those of linear systems.

In a linear optical system, the emergence of EP is independent of the propagation direction of the input field [75,76]. In contrast, the appearance of EP can be nonreciprocal in our nonlinear dissipative system because the different intensities of intracavity fields for opposite-direction inputs can lead to different system dissipation. The transmittance can also be nonreciprocal when input fields are impinged into different WGMRs.

The EPs are the intrinsic property of a linear multimode system. Thus, the input field has no effect on EPs of a linear system [75,76]. However, we find that the input field can modify the property of EPs of a system with nonlinear dissipation. By tuning the input field intensity in a proper range, multiple EPs appear for different frequency detunings between the input field and the cavity mode.

2. System and model

2.1. Coupled-WGMR system

We consider a system consisting of two coupled WGMRs (WGMR1 and WGMR2). The intracavity mode $\hat{a}_1$ ($\hat{a}_2$) with frequency ω_1 (ω_2) of WGMR1 (WGMR2) couples to the lower (upper) waveguide with a strength κ_{c1} (κ_{c2}), shown in Fig. 1. The two modes $\hat{a}_1$ and $\hat{a}_2$ couple to each other with a strength κ_c and decay linearly with rates γ_1 and γ_2, due to either single-photon absorption or side leakage. Meanwhile, we assume that there is nonlinear dissipation in WGMR1 with rate γ_{NL} and this dissipation increases with the intracavity photon intensity. For example, nonlinear dissipation with tunable γ_{NL} can be implemented by two photon absorption of materials consisting of three-level ladder-type atoms [73,77,78]. The two-photon absorption master equation can be described by $\frac{d\hat{\rho}}{dt} = \gamma_{NL}(2\hat{a}_1^2\hat{\rho}\hat{a}_1^\dagger - \hat{a}_1^\dagger\hat{a}_1^2\hat{\rho} - \hat{\rho}\hat{a}_1^\dagger\hat{a}_1^2)$ [77–79], where $\hat{\rho}$ is the corresponding density operator.

Following the quantum jump method used to describe the one-photon loss process presented by Ref. [1], the effective Hamiltonian of the coupled-WGMR system in the rotating frame, with respect to an input field with frequency ω_d, takes the following form ($\hbar = 1$) [2,80]

$$\begin{aligned}\hat{H} = &[\Delta_1 - i(\gamma_1 + \kappa_{c1})]\hat{a}_1^\dagger\hat{a}_1 + [\Delta_2 - i(\gamma_2 + \kappa_{c2})]\hat{a}_2^\dagger\hat{a}_2 - i\gamma_{NL}(\hat{a}_1^\dagger)^2\hat{a}_1^2 \\ &+ \kappa_c(\hat{a}_1^\dagger\hat{a}_2 + \hat{a}_1\hat{a}_2^\dagger) + i\sqrt{2\kappa_{c1}}a_{in}(\hat{a}_1 - \hat{a}_1^\dagger)\,,\end{aligned} \tag{1}$$

where $\Delta_i = \omega_i - \omega_d$ ($i = 1, 2$) is the detuning between the resonance frequency ω_i and the input field frequency ω_d. The input field $a_{\rm in}$ probes the WGMR1 mode $\hat{a}_1$. The corresponding input field intensity is $p_{in} = |a_{in}|^2$.

Optics EXPRESS

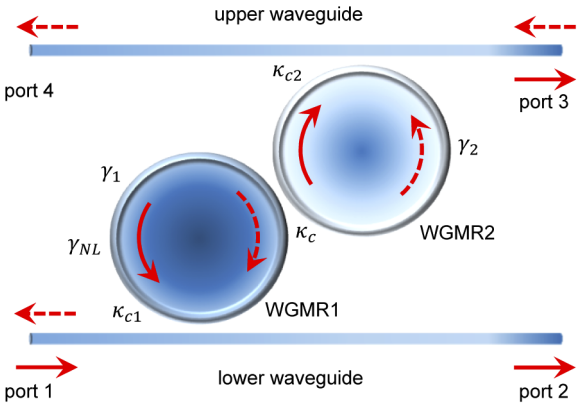

Fig. 1. Schematics of coupled WGMRs. Solid (dashed) arrows represent the transmission of an input field impinging in port 1 (port 3). κ_c is the coupling strength between two WGMRs. κ_{c1} and κ_{c2} are coupling losses of WGMR1 and WGMR2 that are introduced by lower and upper waveguides, respectively. γ_1 (γ_2) represents the linear part of losses of WGMR1 (WGMR2). γ_{NL} represents the nonlinear loss of WGMR1.

The quantum Langevin equations describing the coupled-WGMR system are [2,48]

$$\begin{aligned}\frac{d\hat{a}_1}{dt} &= -i[\Delta_1 - i(\gamma_1 + \kappa_{c1})]\hat{a}_1 - 2\gamma_{NL}\hat{a}_1^{\dagger}\hat{a}_1^2 - i\kappa_c\hat{a}_2 - \sqrt{2\kappa_{c1}}a_{in} \\ &\quad - \sqrt{2\kappa_{c1}}\hat{c}_1^{in} - \sqrt{2\gamma_1}\hat{c}_2^{in} - 2\sqrt{2\gamma_{NL}}\hat{c}_3^{in},\end{aligned} \tag{2}$$

$$\frac{d\hat{a}_2}{dt} = -i[\Delta_2 - i(\gamma_2 + \kappa_{c2})]\hat{a}_2 - i\kappa_c\hat{a}_1 - \sqrt{2\kappa_{c2}}\hat{c}_4^{in} - \sqrt{2\gamma_2}\hat{c}_5^{in}. \tag{3}$$

Here $\hat{c}_1^{in}$ and $\hat{c}_4^{in}$ are noises entering from lower and upper input-output waveguides, whereas $\hat{c}_2^{in}$, $\hat{c}_3^{in}$, and $\hat{c}_5^{in}$ are noises entering from dissipative reservoirs [48]. These noise operators satisfy $\langle\hat{c}_i^{in}(t)\rangle$=0 and $\langle\hat{c}_i^{in\dagger}(t)\hat{c}_i^{in}(t')\rangle = \bar{n}_i^{th}\delta(t-t')$ for reservoirs in thermal equilibrium [2]. Furthermore, at optical frequencies and practical laboratory temperatures, the thermal photon number $\bar{n}_i^{in} = \langle\hat{c}_i^{in\dagger}\hat{c}_i^{in}\rangle$ for (i=1,2,3,4,5) is completely negligible [2]. We can describe the dynamics of $\hat{a}_1$ and $\hat{a}_2$ by that of the corresponding expectation amplitudes.

Taking the average of Eqs. (2) and (3) and defining the expectation amplitudes $a_i = \langle\hat{a}_i\rangle (i = 1, 2)$ [48], we can rewrite Eqs. (2) and (3) describing the dynamics in two coupled WGMRs in the matrix form as follows:

$$\begin{aligned}\frac{d}{dt}\begin{pmatrix} a_1 \\ a_2 \end{pmatrix} &= -i\begin{pmatrix} \Delta_1 - i(\gamma_1 + \kappa_{c1} + 2\gamma_{NL}n_1) & \kappa_c \\ \kappa_c & \Delta_2 - i(\gamma_2 + \kappa_{c2}) \end{pmatrix}\begin{pmatrix} a_1 \\ a_2 \end{pmatrix} - \sqrt{2\kappa_{c1}}\begin{pmatrix} a_{in} \\ 0 \end{pmatrix} \\ &= -iM\begin{pmatrix} a_1 \\ a_2 \end{pmatrix} - \sqrt{2\kappa_{c1}}\begin{pmatrix} a_{in} \\ 0 \end{pmatrix}.\end{aligned} \tag{4}$$

Here we assume the intracavity photon number in WGMR1 is a variable

$$n_1 = \langle\hat{a}_1^{\dagger}\hat{a}_1\rangle = |a_1|^2, \tag{5}$$

since this can qualitatively show its influence and parameter dependence on the property of this coupled system. The expressions containing the variable n_1 below are just formal solutions [66]

Optics EXPRESS

and their values should be obtained by replacing n_1 with $|a_1|^2$ after numerically solving Eq. (4) or its counterpart when probing the linear WGMR2 from port 3.

The characteristic equation and the eigenfrequencies of the coupled-WGMR system can be found from $|\omega I - M| = 0$ [75,76]. The eigenfrequencies of two supermodes due to the coupling of the two WGMRs are as follows:

$$\omega_{\pm} = \frac{1}{2}[\Delta_+ - i\Gamma_+ \pm \sqrt{(\Delta_- - i\Gamma_-)^2 + 4\kappa_c^2}] \,, \tag{6}$$

with

$$\Gamma_{\pm} = (\gamma_1 + \kappa_{c1} + 2\gamma_{NL} n_1) \pm (\gamma_2 + \kappa_{c2}) \,, \tag{7}$$

where $\Delta_{\pm} = \Delta_1 \pm \Delta_2$. Γ_+ and Γ_- denote the sum of loss and the loss contrast of the two WGMRs. In principle, this method is identical to that adopting a proper ansatz with $(a_1, a_2)^T = (a_1', a_2')^T \exp(-i\omega t)$ and substituting it into Eq. (4) [67]. Furthermore, the term with the square-root represents either the frequency splitting (i.e., in the PT unbroken phase) or the linewidth modification (i.e., in the PT broken phase) due to the coupling between two WGMRs. When the two WGMRs are on resonance that $\Delta_1 = \Delta_2 = \Delta_0$, the eigenfrequencies of two supermodes are reduced to

$$\omega_{\pm} = \Delta_0 - \frac{i\Gamma_+ \mp \sqrt{4\kappa_c^2 - \Gamma_-^2}}{2} \,. \tag{8}$$

Here, the square-root $\sqrt{4\kappa_c^2 - \Gamma_-^2}$ is real for $2\kappa_c - \Gamma_- > 0$ or imaginary for $2\kappa_c - \Gamma_- < 0$, taking $\Gamma_- \geq 0$. At $2\kappa_c - \Gamma_- = 0$, the eigenstates and complex eigenfrequencies (ω_+ and ω_-) simultaneously coalesce. Therefore, the system is in a non-Hermitian degeneracy and EP appears. According to Eq. (7), the EP is crucially dependent on the intracavity photon number n_1 in WGMR1.

To derive the transmission amplitudes, we focus on the steady-state solutions of Eq. (4), i.e. $\frac{da_1}{dt} = \frac{da_2}{dt} = 0$, and obtain

$$\begin{aligned} a_1 &= -\frac{\sqrt{2\kappa_{c1}}[i\Delta_2 + (\gamma_2 + \kappa_{c2})]a_{in}}{[i\Delta_1 + (\gamma_1 + \kappa_{c1}) + 2\gamma_{NL} n_1][i\Delta_2 + (\gamma_2 + \kappa_{c2})] + \kappa_c^2} \,, \\ a_2 &= i\frac{\kappa_c \sqrt{2\kappa_{c1}} a_{in}}{[i\Delta_1 + (\gamma_1 + \kappa_{c1}) + 2\gamma_{NL} n_1][i\Delta_2 + (\gamma_2 + \kappa_{c2})] + \kappa_c^2} \,. \end{aligned} \tag{9}$$

Furthermore, we use the input-output relations for WGMR1 and WGMR2 and obtain $a_{out2} = a_{in} + \sqrt{2\kappa_{c1}} a_1$ and $a_{out3} = \sqrt{2\kappa_{c2}} a_2$. We have the transmittance $T_{1\to2}$ ($T_{1\to3}$) of this system from the input port 1 to the output port 2 (port 3) as follows:

$$T_{1\to2} = \left| 1 - \frac{2\kappa_{c1}[i\Delta_2 + (\gamma_2 + \kappa_{c2})]}{[i\Delta_1 + (\gamma_1 + \kappa_{c1}) + 2\gamma_{NL} n_1][i\Delta_2 + (\gamma_2 + \kappa_{c2})] + \kappa_c^2} \right|^2 , \tag{10}$$

$$T_{1\to3} = \left| \frac{2\kappa_c \sqrt{\kappa_{c1}\kappa_{c2}}}{[i\Delta_1 + (\gamma_1 + \kappa_{c1}) + 2\gamma_{NL} n_1][i\Delta_2 + (\gamma_2 + \kappa_{c2})] + \kappa_c^2} \right|^2 . \tag{11}$$

Here $T_{1\to2}$ represents the direct transmittance of the case that the output field and input field are in the lower waveguide, while $T_{1\to3}$ represents the cross transmittance of the case that the output field and input field are in different waveguides. These transmittances depend on the linear loss and the coupling strength κ_c as in a linear system [35], together with the intracavity photon number n_1 in WGMR1 and the two-photon absorption coefficient γ_{NL}. Therefore, in contrast to a linear system, tuning the input field intensity or frequency can significantly change the transmittances of this coupled-WGMR system with nonlinear dissipation even when all system parameters are fixed.

Optics EXPRESS

Now we consider the case that the input field is impinged in the upper waveguide and probes WGMR2 ($\hat{a}_{2'}$) other than WGMR1 ($\hat{a}_{1'}$). The effective Hamiltonian describing this coupled-WGMR system takes the form

$$\begin{aligned}\hat{H}' = &[\Delta_1 - i(\gamma_1 + \kappa_{c1})]\hat{a}_{1'}^{\dagger}\hat{a}_{1'} + [\Delta_2 - i(\gamma_2 + \kappa_{c2})]\hat{a}_{2'}^{\dagger}\hat{a}_{2'} - i\gamma_{NL}(\hat{a}_{1'}^{\dagger})^2\hat{a}_{1'}^2, \\ &+ \kappa_c(\hat{a}_{1'}^{\dagger}\hat{a}_{2'} + \hat{a}_{1'}\hat{a}_{2'}^{\dagger}) + i\sqrt{2\kappa_{c2}}a_{in}(\hat{a}_{2'} - \hat{a}_{2'}^{\dagger}).\end{aligned} \tag{12}$$

The form of $\hat{H}'$ is identical to that of $\hat{H}$ in which the input field probes WGMR1, except the last term representing the probing on WGMR2.

The equations describing the dynamics of the two coupled WGMRs are

$$\frac{d}{dt}\begin{pmatrix} a_{1'} \\ a_{2'} \end{pmatrix} = -i\begin{pmatrix} \Delta_1 - i(\gamma_1 + \kappa_{c1} + 2\gamma_{NL}n_{1'}) & \kappa_c \\ \kappa_c & \Delta_2 - i(\gamma_2 + \kappa_{c2}) \end{pmatrix}\begin{pmatrix} a_{1'} \\ a_{2'} \end{pmatrix} - \sqrt{2\kappa_{c2}}\begin{pmatrix} 0 \\ a_{in} \end{pmatrix}. \tag{13}$$

Here we define the mode amplitudes $a_{i'} = \langle \hat{a}_{i'} \rangle (i = 1, 2)$ and have the intracavity field intensity in WGMR1 as a variable

$$n_{1'} = \langle \hat{a}_{1'}^{\dagger}\hat{a}_{1'} \rangle = |a_{1'}|^2 . \tag{14}$$

Following a procedure similar to that shown above and taking the input-output relations of $a_{out4} = a_{in} + \sqrt{2\kappa_{c2}}a_{2'}$ and $a_{out1} = \sqrt{2\kappa_{c1}}a_{1'}$, the cavity modes $a_{1'}$ and $a_{2'}$ can be derived in steady state as

$$a_{1'} = i\frac{\kappa_c\sqrt{2\kappa_{c2}}a_{in}}{[i\Delta_1 + (\gamma_1 + \kappa_{c1}) + 2\gamma_{NL}n_{1'}][i\Delta_2 + (\gamma_2 + \kappa_{c2})] + \kappa_c^2} , \tag{15}$$

$$a_{2'} = -\frac{\sqrt{2\kappa_{c2}}[i\Delta_1 + (\gamma_1 + \kappa_{c1} + 2\gamma_{NL}n_{1'})]a_{in}}{[i\Delta_1 + (\gamma_1 + \kappa_{c1}) + 2\gamma_{NL}n_{1'}][i\Delta_2 + (\gamma_2 + \kappa_{c2})] + \kappa_c^2} . \tag{16}$$

The corresponding transmittances are

$$T_{3\to4} = \left|1 - \frac{2\kappa_{c2}[i\Delta_1 + (\gamma_1 + \kappa_{c1} + 2\gamma_{NL}n_{1'})]}{[i\Delta_1 + (\gamma_1 + \kappa_{c1}) + 2\gamma_{NL}n_{1'}][i\Delta_2 + (\gamma_2 + \kappa_{c2})] + \kappa_c^2}\right|^2 , \tag{17}$$

$$T_{3\to1} = \left|\frac{2\kappa_c\sqrt{\kappa_{c1}\kappa_{c2}}}{[i\Delta_1 + (\gamma_1 + \kappa_{c1}) + 2\gamma_{NL}n_{1'}][i\Delta_2 + (\gamma_2 + \kappa_{c2})] + \kappa_c^2}\right|^2 , \tag{18}$$

where $T_{3\to4}$ ($T_{3\to1}$) represents the transmittance from the input port 3 to the output port 4 (port 1). Clearly, the direct transmittance $T_{3\to4}$ is different from its counterpart $T_{1\to2}$ obtained when the input field probes WGMR1. Meanwhile, although the expressions of the cross transmittances $T_{1\to3}$ and $T_{3\to1}$ are the same, $T_{1\to3}$ and $T_{3\to1}$ can also be different because the intracavity photon number in WGMR1 for these two cases are different, due to the asymmetric intracavity intensity distribution and the two-photon absorption.

2.2. Nonreciprocal EPs

For studying the influence of the input field on the EPs, one waveguide is decoupled from the corresponding WGMR [35]. In the following section, we specify the case that the upper waveguide was moved away, while the other case can be described in a similar way.

After decoupling the interaction between the upper waveguide and WGMR2, the eigenfrequencies of this simplified coupled-WGMR system can be obtained from Eq. (6) by setting $\kappa_{c2} = 0$. Without loss of generality, the resonant frequencies and linear losses of two WGMRs are tuned

Optics EXPRESS

to be equal with $\Delta_1 = \Delta_2 = \Delta_0$ and $\gamma_1 = \gamma_2 = \gamma_0$, respectively. The eigenfrequencies can be described as

$$\omega_{\pm} = \Delta_0 - \frac{i(\kappa_{c1} + 2\gamma_0 + 2\gamma_{NL}n_1) \mp \sqrt{4\kappa_c^2 - (\kappa_{c1} + 2\gamma_{NL}n_1)^2}}{2}, \tag{19}$$

which is crucially dependent on intracavity photon number n_1 in WGMR1.

The influence of the intensity and frequency of the input field on the imaginary parts of $\omega_{\pm}$ and thus the appearance of EP is shown in Fig. 2(a). The corresponding intracavity photon number n_1 is shown in Fig. 2(b). Here the coupling between two WGMRs is set to $\kappa_c = 1$, the coupling between WGMR1 and the lower waveguide is $\kappa_{c1} = 1.8$, the linear loss rates of both WGMRs are set to be equal with $\gamma_1 = \gamma_2 = 1$, and the two-photon absorption rate is $\gamma_{NL} = 0.5$.

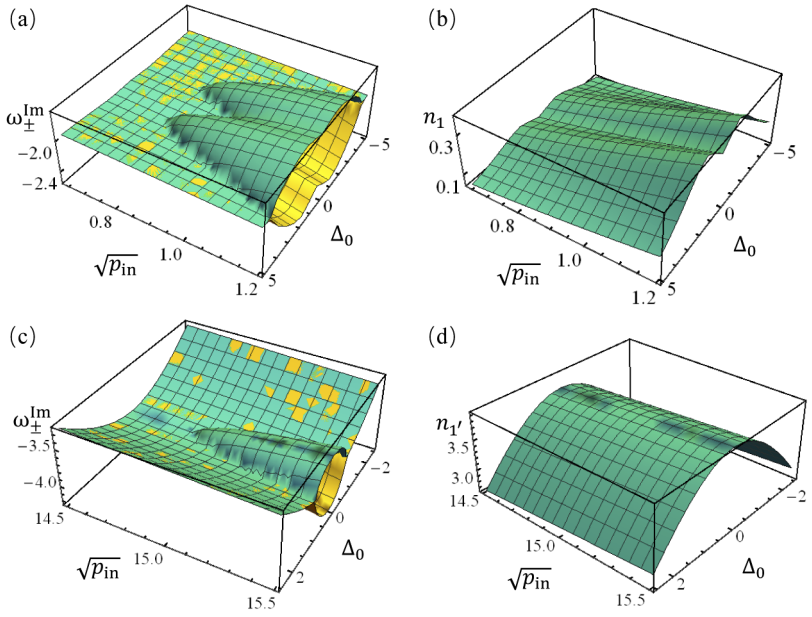

Fig. 2. Imaginary parts of two eigenfrequencies $\omega_{\pm}$ and intracavity photon number in WGMR1 : (a) $\omega_{\pm}^{\mathrm{Im}}$ as a function of the frequency and intensity of input fields impinging in port 1 ($\kappa_{c1} = 1.8$, $\kappa_{c2} = 0$); (b) n_1 as a function of the frequency and intensity of input fields impinging in port 1 ($\kappa_{c1} = 1.8$, $\kappa_{c2} = 0$); (c) $\omega_{\pm}^{\mathrm{Im}}$ as a function of the frequency and intensity of input fields impinging in port 3 ($\kappa_{c1} = 0$, $\kappa_{c2} = 1.8$); (d) $n_{1'}$ as a function of the frequency and intensity of input fields impinging in port 3 ($\kappa_{c1} = 0$, $\kappa_{c2} = 1.8$). Here $\kappa_c = 1.0$, $\gamma_1 = \gamma_2 = 1.0$, and $\gamma_{NL} = 0.5$.

Specifically, we focus on the scattering of four input fields when the upper waveguide is moved away. The imaginary parts $\omega_{\pm}^{\mathrm{Im}}$ of the eigenfrequencies $\omega_{\pm}$ for $\sqrt{p_{in}} \in \{0.7, 0.8, 0.943, 1.0\}$ are shown in the left panel of Fig. 3 with increasing input field intensity from top to bottom. For a weak input field with $\sqrt{p_{in}} = 0.7$, there is no EP when changing the input frequency. For a larger input field with $\sqrt{p_{in}} = 0.8$, there are four EPs and these EPs symmetrically distributed on the two sides of the resonance frequency. This is because that a local minimum of the photon number in WGMR1 is achieved at resonance and its value $n_{1,\Delta_0=0}$ is smaller than a threshold $n_{1,EP} = (\pm 2\kappa_c - \kappa_{c1} - \Gamma_0)/2\gamma_{NL} > 0$ with $\Gamma_0 = \gamma_1 - \gamma_2$ (i.e., $n_{1,EP} = 0.2$ for the parameters used here). However, when the input field intensity is further increased with $\sqrt{p_{in}} = 0.943$, there are only three EPs because $n_{1,\Delta_0=0} = n_{1,EP}$ is achieved. Furthermore, the number of EP decreases to two when the input field intensity increases further with $\sqrt{p_{in}} = 1.0$.

Optics EXPRESS

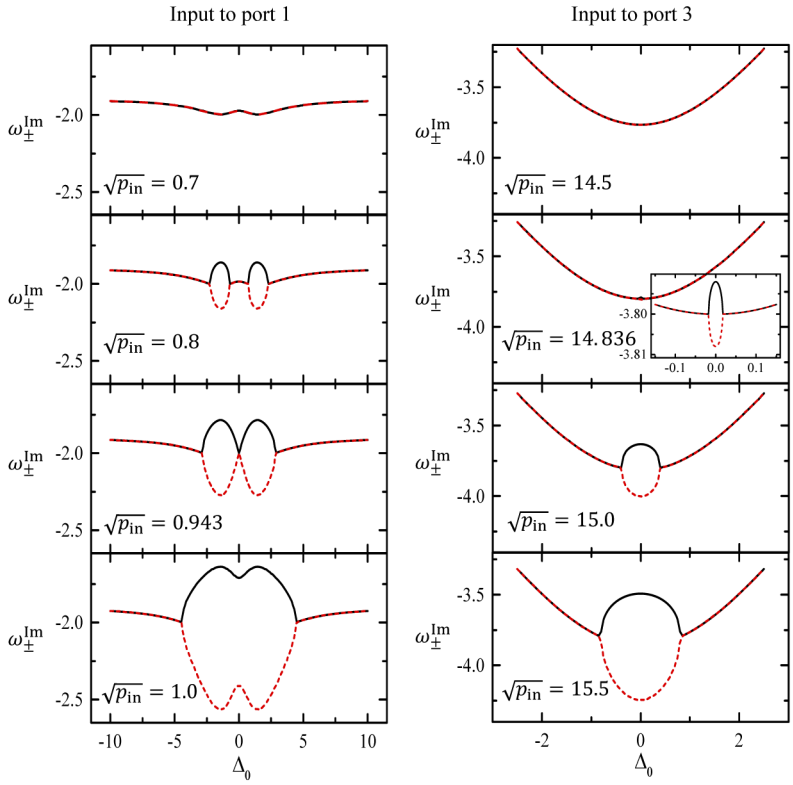

Fig. 3. Imaginary parts $\omega_{\pm}^{\mathrm{Im}}$ of two eigenfrequencies $\omega_{\pm}$. Left panel, $\omega_{\pm}^{\mathrm{Im}}$ as a function of the frequency of input fields impinging in port 1 ($\kappa_{c1} = 1.8$, $\kappa_{c2} = 0$) with different intensities; Right panel, $\omega_{\pm}^{\mathrm{Im}}$ as a function of the frequency of input fields impinging in port 3 ($\kappa_{c1} = 0$, $\kappa_{c2} = 1.8$) with different intensities. Here $\kappa_c = 1.0$, $\gamma_1 = \gamma_2 = 1.0$, and $\gamma_{NL} = 0.5$ are used for both panels.

We include the corresponding functions $\omega_{\pm}^{\mathrm{Im}}$ and $n_{1'}$ in Figs. 2(c) and 2(d) for the case that the lower waveguide other than the upper waveguide is moved away. All parameters are the same as in Figs. 2(a) and 2(b) except the exchange of κ_{c1} and κ_{c2} (i.e., $\kappa_{c1} = 0$ and $\kappa_{c2} = 1.8$). Similarly, we focus on the scattering of four input fields with $\sqrt{p_{in}} \in \{14.5, 14.836, 15.0, 15.5\}$. The imaginary parts $\omega_{\pm}^{\mathrm{Im}}$ of the eigenfrequencies are shown in the right panel of Fig. 3 with increasing input field intensity from top to bottom. For a weak input field impinged in WGMR2, no EP appears when we use the same system parameters as in Figs. 2(c) and 2(d). However, an EP appears at the resonant frequency when the input field intensity is increased to $\sqrt{p_{in}} = 14.836$, and then two EPs appear symmetrically at two detunings with the same magnitude. Therefore, the emergence of EPs and their numbers are dependent on the intensity and frequency of the input field in combination with its direction.

To specify the nonreciprocity of EPs in this system, the imaginary parts $\omega_{\pm}^{\mathrm{Im}}$ of the eigenfrequencies as a function of the coupling strength κ_c and input field intensity $\sqrt{p_{in}}$ are shown in Fig. 4(a) and 4(b) for the cases that the upper and lower waveguide is moved away, respectively. Here we assumed that the input field is resonant with the WGMRs and that all the other parameters in Fig. 4(a) and 4(b) are the same as in Fig. 2(a) and Fig. 2(c), respectively. The condition of EP appearance for the two cases is notably different from each other, leading to the nonreciprocity of EPs. Furthermore, we showed the evolution of $\omega_{\pm}^{\mathrm{Im}}$ using the resonant input field with critical intensity as κ_c was increased in Fig. 4(c) and 4(d). For the case that the upper waveguide is

Optics EXPRESS

moved away, there is only one EP, shown in Fig. 4(c), when we change the coupling strength κ_c using a resonant input field with the critical intensity $\sqrt{p_{in}} = 0.943$. Meanwhile, the EP appears at $\kappa_c = 1$, which is in coincidence with Fig. 2(a). However, for the case that the lower waveguide is moved away and the input field probes WGMR2, there are three EPs, shown in Fig. 4(d), when changing κ_c using a resonant input field with the critical intensity $\sqrt{p_{in}} = 14.836$. Note that one EP appears at $\kappa_c = 1$, while the other two EPs appear due to the balance of the coupling strength κ_c and the nonlinear loss $2\gamma_{NL}n_{1'}$ in WGMR1.

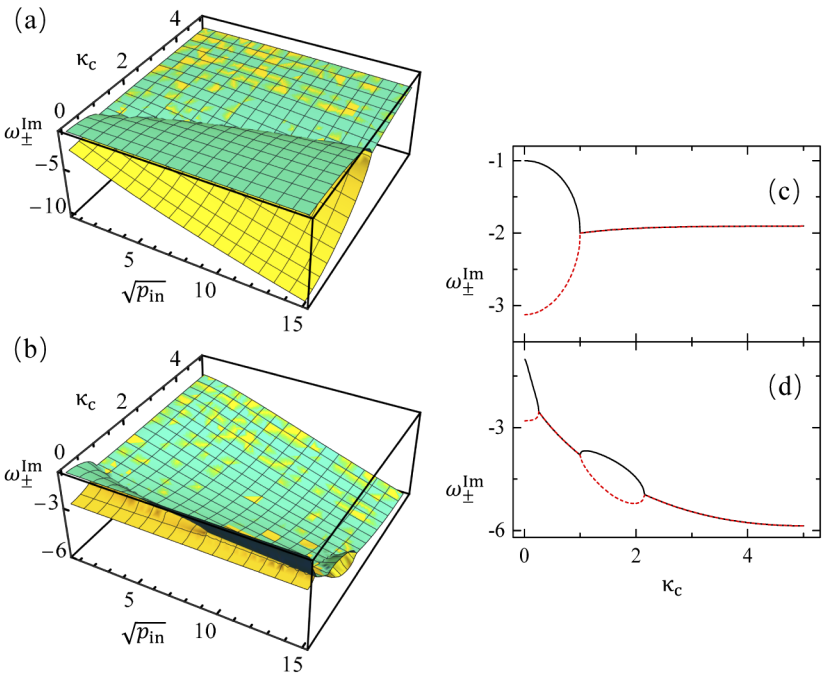

Fig. 4. Imaginary parts $\omega_\pm^{Im}$ of two eigenfrequencies $\omega_\pm$. (a) $\omega_\pm^{Im}$ as a function of the coupling rate κ_c and input field intensity for input fields impinging in port 1 ($\kappa_{c1} = 1.8$, $\kappa_{c2} = 0$); (b) $\omega_\pm^{Im}$ as a function of the coupling rate κ_c and input field intensity for input fields impinging in port 3 ($\kappa_{c1} = 0$, $\kappa_{c2} = 1.8$); (c and d) $\omega_\pm^{Im}$ as a function of the coupling rate κ_c for input fields impinging in port 1 (c) and port 3 (d). The input field intensities in (c) and (d) are tuned to near the critical values that lead to the emergence of an EP at $\kappa_c = 1$ for $\Delta_0 = 0$, respectively.

2.3. *Field-dependent transmission*

In practice, it is hard to directly measure the photon number distribution in WGMR1. However, this distribution is correlated to the transmittance of the coupled-WGMR system, because the transmittance is a constant when the coupled system with nonlinear dissipation is in a steady state and it can be obtained from the input-output relation involving the intracavity mode of WGMRs. For instance, n_1 is correlated to the transmittance $T_{1\to2}$ of this coupled-WGMR system with the input-output relation $a_{out2} = a_{in} + \sqrt{2\kappa_{c1}}a_1$, when the upper waveguide is moved away. Specifically, it can be expressed as [35]

$$n_1 = \frac{T_{1\to2} - 2\sqrt{T_{1\to2}}\cos\theta + 1}{2\kappa_{c1}} p_{in}, \tag{20}$$

Optics EXPRESS

where θ represents the phase of the complex coefficient of amplitude transmission $a_{out2}/a_{in} = \sqrt{T_{1\to2}}e^{i\theta}$ and $p_{in} = |a_{in}|^2$. In contrast to a constant transmittance of linear systems [35], the transmittance $T_{1\to2}$ changes for different input fields and thus depends on n_1, whereas $T_{1\to2}$ for a given input field can be obtained by a measurement and its formal expression can be derived from Eq. (10) as

$$T_{1\to2} = \left|1 - \frac{2\kappa_{c1}(i\Delta_0 + \gamma_0)}{(i\Delta_0 + \gamma_0 + \kappa_{c1} + 2\gamma_{NL}n_1)(i\Delta_0 + \gamma_0) + \kappa_c^2}\right|^2. \tag{21}$$

Therefore, the photon number distribution in WGMR1 can also be written as

$$n_1 = \frac{(\Delta_0^2 - \kappa_c^2 - \gamma_0^2)T_- + \kappa_{c1}\gamma_0 T_+ - (\kappa_{c1} + 2\gamma_0)\Delta_0\sqrt{T_{1\to2}}\sin\theta}{2\kappa_{NL}(\gamma_0 T_- + \Delta_0\sqrt{T_{1\to2}}\sin\theta)}, \tag{22}$$

which is implicitly dependent on the input field intensity and $T_\pm = 1 \pm \sqrt{T_{1\to2}}\cos\theta$. From the formal expression of $T_{1\to2}$ as shown in Eq. (21), it is easily to show that for a resonant input field with Δ_0, an increase of the photon number n_1 in WGMR1 increases the transmittance $T_{1\to2}$, even though the total loss $\Gamma_+ = 2\gamma_0 + \kappa_{c1} + 2\gamma_{NL}n_1$ of the coupled-WGMR system increases linearly with n_1.

Figure 5 shows the transmittance $T_{1\to2}$ as a function of the frequency and intensity of an input field. All parameters are the same as in Fig. 2(a). For a resonant input field with $\Delta_0 = 0$, the transmittance $T_{1\to2}$ increases when the intensity p_{in} increases. For a non-resonant input field (e.g., $|\Delta_0|>1.5$), the transmittance $T_{1\to2}$ first decreases to a minimum and then increases when p_{in} increases. Meanwhile, the coupled-WGMR system is changed from a strong coupling regime ($p_{in}<p'_{in}$) to a weak coupling regime ($p_{in}>p'_{in}$). Here p'_{in} is the input field intensity required to achieve the EP.

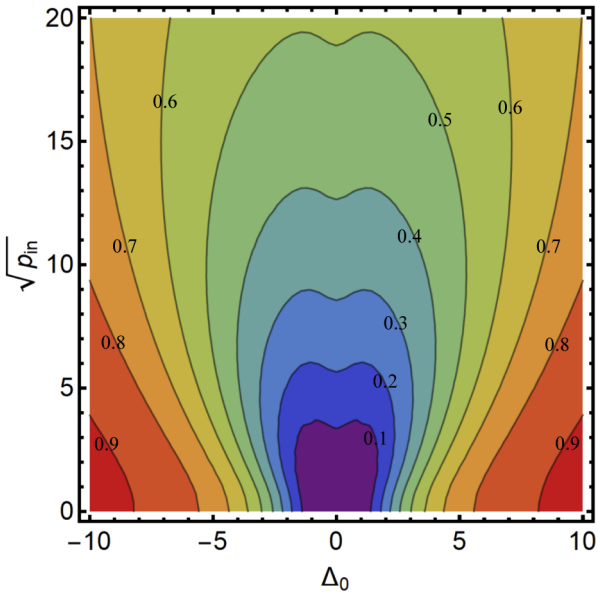

Fig. 5. Transmittance $T_{1\to2}$ as a function of the frequency and intensity of input fields. Here $\kappa_c = 1.0$, $\kappa_{c1} = 1.8$, $\kappa_{c2} = 0$, $\gamma_1 = \gamma_2 = 1.0$, and $\gamma_{NL} = 0.5$.

However, for a given p_{in}, the transmittance $T_{1\to2}$ first decreases to two local minimums and then increases to a local maximum at the resonant point when continuously decreasing $|\Delta_0|$. This

Optics EXPRESS

is inverse to the relation between the intracavity number and the detuning, shown in Fig. 2(b). Therefore, the transmittance $T_{1\to2}$ performs differently when either the intensity or frequency of an input field is changed for a given coupled-WGMR system. This field-dependent property leads to the nonreciprocal transmission of our coupled-WGMR system.

2.4. Nonreciprocal transmission

In this section, we study the scattering process of a coupled-WGMR system, in which nonreciprocal transmission can be achieved when an input field with the same frequency and intensity is impinged into different WGMRs, shown in Fig. 6. The lower and upper waveguides couple to WGMR1 and WGMR2 with identical coupling rates $\kappa_{c1} = \kappa_{c2}$, respectively. The coupling rate between two WGMRs are set to be unity with $\kappa_c = 1$. For simplicity, we study a specified system in which the linear loss of each WGMR is equal to 0.1 and the nonlinear two-photon absorption rate is $\gamma_{NL} = 0.5$. We will show that an input field impinging into port 3 will be output into two ports with an equal intensity (i.e., $T_{3\to4} = T_{3\to1}$) and that an input field impinging into port 1 will be output into the direct transmission mode with vanishing cross transmission (i.e., $T_{1\to3}>0$, $T_{1\to2} \simeq 0$). This can be referred to as nonreciprocal transmission [81–88].

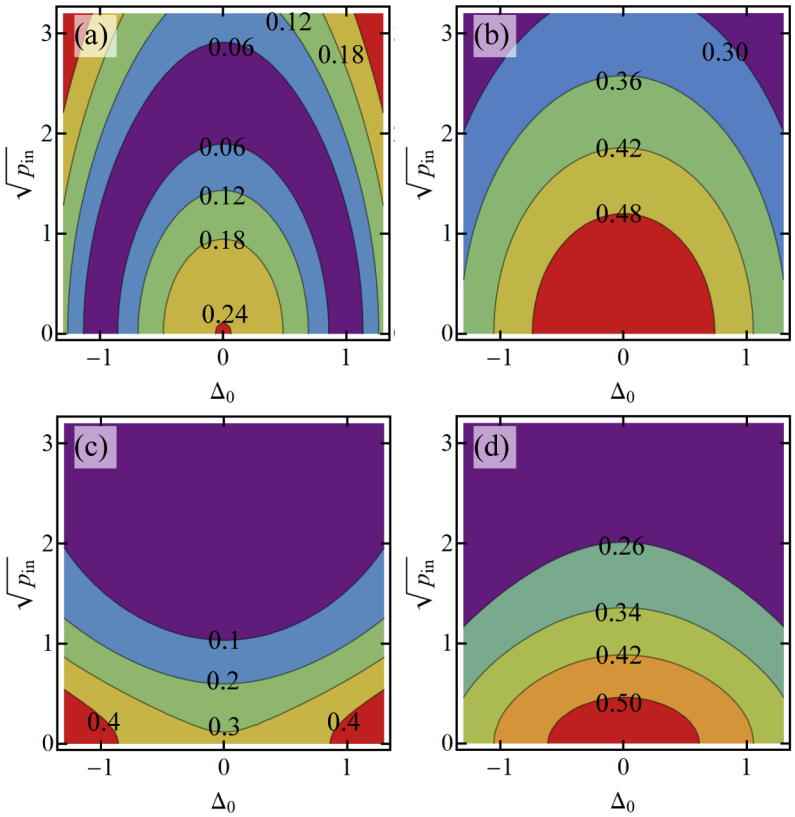

Fig. 6. Transmittances as a function of the frequency and intensity of input fields: (a) $\Delta_T = |T_{3\to1} - T_{3\to4}|$ represents the transmittance difference when impinging the input field in the port 3; (b) $T_{3\to1}$ represents the transmittance into port 1 when impinging the input field in the port 3; (c) $T_{1\to2}$ represents the transmittance into port 2 when impinging the input field in the port 1; (d) $T_{1\to3}$ represents the transmittance into port 3 when impinging the input field in the port 1. Here $\kappa_c = 1.0$, $\kappa_{c1} = \kappa_{c2} = 2.0$, $\gamma_1 = \gamma_2 = 0.1$, and $\gamma_{NL} = 0.5$.

Optics EXPRESS

When the input field probes WGMR2 from port 3, the transmittances $T_{3\to1}$ and $T_{3\to4}$ of this coupled-WGMR system are described in Eq. (17) and (18). The transmittance difference $\Delta_T = |T_{3\to1} - T_{3\to4}|$ as a function of the frequency and intensity of the input field is shown in Fig. 6(a). Meanwhile, the transmittance $T_{3\to1}$ with the same system parameters is shown in Fig. 6(b). There exist a regime labeled in purple in Fig. 6(a) in which an input field is output into the direct transmission (port 4) and cross transmission (port 1) modes with balanced intensities ($\Delta_T \leq 0.06$); the transmittances $T_{3\to1}$ and $T_{3\to4}$ are almost equal and can be as large as 0.40.

When the input field probes WGMR1 from port 1, the corresponding transmittances $T_{1\to3}$ and $T_{1\to2}$ are described in Eq. (10) and (11). Figures 6(c) and 6(d) show the transmittances $T_{1\to3}$ and $T_{1\to2}$ as a function of the frequency and intensity of the input field, respectively. For a given input field frequency, the transmittances $T_{1\to2}$ and $T_{1\to3}$ both continuously decreases when increasing the input field intensity p_{in} with $\sqrt{p_{in}} \in (0, 3.0)$. For a given intensity, however, the transmittances $T_{1\to2}$ and $T_{1\to3}$ change in opposite ways when increasing the frequency detunings $|\Delta_0|$, i.e., $T_{1\to2}$ increases continuously, while $T_{1\to3}$ decreases when $|\Delta_0|$ increases. For the regime where both $|\Delta_T|$ in Fig. 6(a) and $T_{1\to2}$ in Fig. 6(c) approach zero, $T_{1\to3}$ can be larger than 0.30. Therefore, the transmission of this coupled-WGMR system is nonreciprocal and divergent in this regime: An input field is output into the cross transmission mode when it probes WGMR1, while it is equally output into the direct transmission and cross transmission modes when it probes WGMR2.

3. Discussion and summary

So far, we have focused on the nonreciprocal EP and the nonreciprocal transmission of a single probe field. Shi et al. found that the existence of dynamic reciprocity makes optical isolators involving nonlinear processes fail to provide isolation for arbitrary backward-propagating noise coexisting with a forward probe [89]. Although this dynamic reciprocity might present in our coupled-WGMR system involving nonlinear dissipation, nonlinear nonreciprocity presented in the situation with a single probe is still useful for practical applications, such as nonlinear nonreciprocal devices [90–93].

The nonlinear dissipation is the main reason leading to nonreciprocal EPs and transmission. The nonlinear loss due to two-photon absorption modifies the total loss of WGMR1 and increases linearly with the increase of the average photon number in WGMR1. Parameters being capable of tuning n_1 have influence on the emergence of EP. By decoupling WGMR2 (WGMR1) from the upper (lower) waveguide, i.e. $\kappa_{c2} = 0$ ($\kappa_{c1} = 0$), we showed that the number of EPs can vary significantly when the frequency and intensity of the probe field change. The EPs appear in a nonreciprocal pattern when probing different WGMRs (see Fig. 3) . This might be useful for studying the interesting EP-based applications [14–25]. Furthermore, in our nonlinear dissipative system, a probe field with different intensities or frequencies leads to different intracavity intensities and thus different total losses in WGMR1. As a result, the nonreciprocal transmission is also influenced by the nonlinear two-photon absorption.

Currently, two-photon absorption of natural material is small, while it requires a large two-photon absorption to achieve a high performance of the present protocol for a low intensity input field. In principle, large two-photon absorption nonlinearity can be achieved by using atomic ensembles with two-photon transmission [73]. Furthermore, for a finite two-photon absorption, our protocols can work when high-intensity input fields are impinged into this system, because the extra loss of WGMR1 proportional to $2\gamma_{NL}n_1$ or $2\gamma_{NL}n_{1'}$ is the main factor influencing the transmittances and the emergence of EP.

In summary, we have shown that nonreciprocal EPs can be induced by nonlinear dissipation in a coupled-WGMR system. Due to the nonlinearity, the condition of nonreciprocal EPs emerging and EP number are dependent on the intensity and frequency of the input field. Meanwhile, the system transmits an input field in a nonreciprocal way, directing the input field probing the linear WGMR into two outputs equally and that probing the nonlinear WGMR primarily into one

Optics EXPRESS

output. This nonlinear system may be used to study optical nonreciprocity at EPs and to explore EP-based applications.

Funding. National Key Research and Development Program of China (2017YFA0303703, 2019YFA0308700, 2019YFA0308704); Natural Science Foundation of Jiangsu Province (BK20180461); National Natural Science Foundation of China (11874212, 11890704, 11904171).

Disclosures. The authors declare no conflicts of interest.

Data availability. Data underlying the results presented in this paper are not publicly available at this time but may be obtained from the authors upon reasonable request.

References

1. M. B. Plenio and P. L. Knight, "The quantum-jump approach to dissipative dynamics in quantum optics," Rev. Mod. Phys. **70**(1), 101–144 (1998).
2. H. J. Carmichael, *Statistical Methods in Quantum Optics 1: Master Equations and Fokker-Planck Equations* (Springer, 1999).
3. C. M. Bender, "Making sense of non-Hermitian Hamiltonians," Rep. Prog. Phys. **70**(6), 947–1018 (2007).
4. R. El-Ganainy, K. G. Makris, M. Khajavikhan, Z. H. Musslimani, S. Rotter, and D. N. Christodoulides, "Non-Hermitian physics and PT symmetry," Nat. Phys. **14**(1), 11–19 (2018).
5. W. D. Heiss, "Exceptional points of non-Hermitian operators," J. Phys. A: Math. Gen. **37**(6), 2455–2464 (2004).
6. V. Dominguez-Rocha, R. Thevamaran, F. M. Ellis, and T. Kottos, "Environmentally induced exceptional points in elastodynamics," Phys. Rev. Appl. **13**(1), 014060 (2020).
7. F. Minganti, A. Miranowicz, R. W. Chhajlany, and F. Nori, "Quantum exceptional points of non-Hermitian Hamiltonians and Liouvillians: The effects of quantum jumps," Phys. Rev. A **100**(6), 062131 (2019).
8. S. X. Li, X. Q. Zhang, Q. Xu, M. Liu, M. Kang, J. G. Han, and W. L. Zhang, "Exceptional point in a metal-graphene hybrid metasurface with tunable asymmetric loss," Opt. Express **28**(14), 20083–20094 (2020).
9. P. C. Kuo, N. Lambert, A. Miranowicz, H. B. Chen, G. Y. Chen, Y. N. Chen, and F. Nori, "Collectively induced exceptional points of quantum emitters coupled to nanoparticle surface plasmons," Phys. Rev. A **101**(1), 013814 (2020).
10. I. Arkhipov, A. Miranowicz, F. Minganti, and F. Nori, "Quantum and semiclassical exceptional points of a linear system of coupled cavities with losses and gain within the Scully-Lamb laser theory," Phys. Rev. A **101**(1), 013812 (2020).
11. N. Habler and J. Scheuer, "Higher-order exceptional points: A route for flat-top optical filters," Phys. Rev. A **101**(4), 043828 (2020).
12. J. Wen, C. Zheng, X. Kong, S. Wei, T. Xin, and G. Long, "Experimental demonstration of a digital quantum simulation of a general $\mathcal{PT}$-symmetric system," Phys. Rev. A **99**(6), 062122 (2019).
13. W.-C. Gao, C. Zheng, L. Liu, T.-J. Wang, and C. Wang, "Experimental simulation of the parity-time symmetric dynamics using photonic qubits," Opt. Express **29**(1), 517–526 (2021).
14. J. Wiersig, "Enhancing the sensitivity of frequency and energy splitting detection by using exceptional points: Application to microcavity sensors for single-particle detection," Phys. Rev. Lett. **112**(20), 203901 (2014).
15. M. P. Hokmabadi, A. Schumer, D. N. Christodoulides, and M. Khajavikhan, "Non-Hermitian ring laser gyroscopes with enhanced Sagnac sensitivity," Nature **576**(7785), 70–74 (2019).
16. J. Wiersig, "Prospects and fundamental limits in exceptional point-based sensing," Nat. Commun. **11**(1), 2454 (2020).
17. X. Mao, G.-Q. Qin, H. Yang, H. Zhang, M. Wang, and G.-L. Long, "Enhanced sensitivity of optical gyroscope in a mechanical parity-time-symmetric system based on exceptional point," New J. Phys. **22**(9), 093009 (2020).
18. G. Q. Zhang, Y. P. Wang, and J. Q. You, "Dispersive readout of a weakly coupled qubit via the parity-time-symmetric phase transition," Phys. Rev. A **99**(5), 052341 (2019).
19. H. Jing, S. K. Ozdemir, X. Y. Lu, J. Zhang, L. Yang, and F. Nori, "PT-symmetric phonon laser," Phys. Rev. Lett. **113**(5), 053604 (2014).
20. Z. Lin, H. Ramezani, T. Eichelkraut, T. Kottos, H. Cao, and D. N. Christodoulides, "Unidirectional invisibility induced by PT-symmetric periodic structures," Phys. Rev. Lett. **106**(21), 213901 (2011).
21. L. Feng, Y. L. Xu, W. S. Fegadolli, M. H. Lu, J. E. B. Oliveira, V. R. Almeida, Y. F. Chen, and A. Scherer, "Experimental demonstration of a unidirectional reflectionless parity-time metamaterial at optical frequencies," Nat. Mater. **12**(2), 108–113 (2013).
22. J.-H. Wu, M. Artoni, and G. C. La Rocca, "Non-Hermitian degeneracies and unidirectional reflectionless atomic lattices," Phys. Rev. Lett. **113**(12), 123004 (2014).
23. C. Dembowski, B. Dietz, H. D. Graf, H. L. Harney, A. Heine, W. D. Heiss, and A. Richter, "Encircling an exceptional point," Phys. Rev. E **69**(5), 056216 (2004).
24. H. Xu, D. Mason, L. Y. Jiang, and J. G. E. Harris, "Topological energy transfer in an optomechanical system with exceptional points," Nature **537**(7618), 80–83 (2016).
25. S. Dey, A. Laha, and S. Ghosh, "Nonlinearity-induced anomalous mode collapse and nonchiral asymmetric mode switching around multiple exceptional points," Phys. Rev. B **101**(12), 125432 (2020).

Optics EXPRESS

26. J. Wen, X. Jiang, L. Jiang, and M. Xiao, "Parity-time symmetry in optical microcavity systems," J. Phys. B: At., Mol. Opt. Phys. **51**(22), 222001 (2018).
27. X. Jiang and L. Yang, "Optothermal dynamics in whispering-gallery microresonators," Light: Sci. Appl. **9**(1), 24 (2020).
28. X.-F. Jiang, C.-L. Zou, L. Wang, Q. Gong, and Y.-F. Xiao, "Whispering-gallery microcavities with unidirectional laser emission," Laser Photonics Rev. **10**(1), 40–61 (2016).
29. P.-B. Li, S.-Y. Gao, and F.-L. Li, "Quantum-information transfer with nitrogen-vacancy centers coupled to a whispering-gallery microresonator," Phys. Rev. A **83**(5), 054306 (2011).
30. J. Wiersig, "Structure of whispering-gallery modes in optical microdisks perturbed by nanoparticles," Phys. Rev. A **84**(6), 063828 (2011).
31. B. Peng, S. K. Ozdemir, M. Liertzer, W. J. Chen, J. Kramer, H. Yilmaz, J. Wiersig, S. Rotter, and L. Yang, "Chiral modes and directional lasing at exceptional points," Proc. Natl. Acad. Sci. U. S. A. **113**(25), 6845–6850 (2016).
32. X.-F. Liu, T.-J. Wang, Y.-P. Gao, C. Cao, and C. Wang, "Chiral microresonator assisted by Rydberg-atom ensembles," Phys. Rev. A **98**(3), 033824 (2018).
33. B. Peng, S. K. Ozdemir, F. C. Lei, F. Monifi, M. Gianfreda, G. L. Long, S. H. Fan, F. Nori, C. M. Bender, and L. Yang, "Parity-time-symmetric whispering-gallery microcavities," Nat. Phys. **10**(5), 394–398 (2014).
34. L. Chang, X. S. Jiang, S. Y. Hua, C. Yang, J. M. Wen, L. Jiang, G. Y. Li, G. Z. Wang, and M. Xiao, "Parity-time symmetry and variable optical isolation in active-passive-coupled microresonators," Nat. Photonics **8**(7), 524–529 (2014).
35. B. Peng, S. K. Ozdemir, S. Rotter, H. Yilmaz, M. Liertzer, F. Monifi, C. M. Bender, F. Nori, and L. Yang, "Loss-induced suppression and revival of lasing," Science **346**(6207), 328–332 (2014).
36. F.-J. Shu, C.-L. Zou, X.-B. Zou, and L. Yang, "Chiral symmetry breaking in a microring optical cavity by engineered dissipation," Phys. Rev. A **94**(1), 013848 (2016).
37. F. Yang, Y. C. Liu, and L. You, "Anti-PT symmetry in dissipatively coupled optical systems," Phys. Rev. A **96**(5), 053845 (2017).
38. F. Zhang, Y. Feng, X. Chen, L. Ge, and W. Wan, "Synthetic anti-PT symmetry in a single microcavity," Phys. Rev. Lett. **124**(5), 053901 (2020).
39. A. Calabrese, F. Ramiro-Manzano, H. M. Price, S. Biasi, M. Bernard, M. Ghulinyan, I. Carusotto, and L. Pavesi, "Unidirectional reflection from an integrated "taiji" microresonator," Photonics Res. **8**(8), 1333–1341 (2020).
40. B. He, L. Yang, X. Jiang, and M. Xiao, "Transmission nonreciprocity in a mutually coupled circulating structure," Phys. Rev. Lett. **120**(20), 203904 (2018).
41. H. Zhang, F. Saif, Y. Jiao, and H. Jing, "Loss-induced transparency in optomechanics," Opt. Express **26**(19), 25199–25210 (2018).
42. L. Liu, J. H. Zhang, L. Jin, and L. Zhou, "Transport properties of the non-Hermitian T-shaped quantum router," Opt. Express **27**(10), 13694–13705 (2019).
43. T. Liu, G. C. Ma, S. J. Liang, H. Gao, Z. M. Gu, S. W. An, and J. Zhu, "Single-sided acoustic beam splitting based on parity-time symmetry," Phys. Rev. B **102**(1), 014306 (2020).
44. Z. P. Liu, J. Zhang, S. K. Ozdemir, B. Peng, H. Jing, X. Y. Lu, C. W. Li, L. Yang, F. Nori, and Y. X. Liu, "Metrology with PT-symmetric cavities: Enhanced sensitivity near the PT-phase transition," Phys. Rev. Lett. **117**(11), 110802 (2016).
45. W. J. Chen, S. K. Ozdemir, G. M. Zhao, J. Wiersig, and L. Yang, "Exceptional points enhance sensing in an optical microcavity," Nature **548**(7666), 192–196 (2017).
46. H. Hodaei, A. U. Hassan, S. Wittek, H. Garcia-Gracia, R. El-Ganainy, D. N. Christodoulides, and M. Khajavikhan, "Enhanced sensitivity at higher-order exceptional points," Nature **548**(7666), 187–191 (2017).
47. W. J. Chen, J. Zhang, B. Peng, S. K. Ozdemir, X. D. Fan, and L. Yang, "Parity-time-symmetric whispering-gallery mode nanoparticle sensor invited," Photonics Res. **6**(5), A23–A30 (2018).
48. H. K. Lau and A. A. Clerk, "Fundamental limits and non-reciprocal approaches in non-Hermitian quantum sensing," Nat. Commun. **9**(1), 4320 (2018).
49. M. Zhang, W. Sweeney, C. W. Hsu, L. Yang, A. D. Stone, and L. Jiang, "Quantum noise theory of exceptional point amplifying sensors," Phys. Rev. Lett. **123**(18), 180501 (2019).
50. G. Q. Qin, M. Wang, J. W. Wen, D. Ruan, and G. L. Long, "Brillouin cavity optomechanics sensing with enhanced dynamical backaction," Photonics Res. **7**(12), 1440–1446 (2019).
51. S. N. Huai, Y. L. Liu, J. Zhang, L. Yang, and Y. X. Liu, "Enhanced sideband responses in a PT-symmetric-like cavity magnomechanical system," Phys. Rev. A **99**(4), 043803 (2019).
52. P. Djorwe, Y. Pennec, and B. Djafari-Rouhani, "Exceptional point enhances sensitivity of optomechanical mass sensors," Phys. Rev. Appl. **12**(2), 024002 (2019).
53. Q. Zhong, J. Ren, M. Khajavikhan, D. N. Christodoulides, S. K. Özdemir, and R. El-Ganainy, "Sensing with exceptional surfaces in order to combine sensitivity with robustness," Phys. Rev. Lett. **122**(15), 153902 (2019).
54. Y. H. Lai, Y. K. Lu, M. G. Suh, Z. Q. Yuan, and K. Vahala, "Observation of the exceptional-point-enhanced Sagnac effect," Nature **576**(7785), 65–69 (2019).
55. Z. C. Zhang, Y. P. Wang, and X. G. Wang, "PT-symmetry-breaking-enhanced cavity optomechanical magnetometry," Phys. Rev. A **102**(2), 023512 (2020).

Optics EXPRESS

56. Y. M. Chu, Y. Liu, H. B. Liu, and J. M. Cai, "Quantum sensing with a single-qubit pseudo-Hermitian system," Phys. Rev. Lett. **124**(2), 020501 (2020).
57. L. Feng, Z. J. Wong, R. M. Ma, Y. Wang, and X. Zhang, "Single-mode laser by parity-time symmetry breaking," Science **346**(6212), 972–975 (2014).
58. Z. Lin, A. Pick, M. Loncar, and A. W. Rodriguez, "Enhanced spontaneous emission at third-order Dirac exceptional points in inverse-designed photonic crystals," Phys. Rev. Lett. **117**(10), 107402 (2016).
59. H. Hodaei, M. A. Miri, M. Heinrich, D. N. Christodoulides, and M. Khajavikhan, "Parity-time-symmetric microring lasers," Science **346**(6212), 975–978 (2014).
60. M. Kim, K. Kwon, J. Shim, Y. Jung, and K. Yu, "Partially directional microdisk laser with two Rayleigh scatterers," Opt. Lett. **39**(8), 2423–2426 (2014).
61. P. Miao, Z. F. Zhang, J. B. Sun, W. Walasik, S. Longhi, N. M. Litchinitser, and L. Feng, "Orbital angular momentum microlaser," Science **353**(6298), 464–467 (2016).
62. J. Perina, A. Luks, J. K. Kalaga, W. Leonski, and A. Miranowicz, "Nonclassical light at exceptional points of a quantum PT-symmetric two-mode system," Phys. Rev. A **100**(5), 053820 (2019).
63. E. Lafalce, Q. J. Zeng, C. H. Lin, M. J. Smith, S. T. Malak, J. Jung, Y. J. Yoon, Z. Q. Lin, V. V. Tsukruk, and Z. V. Vardeny, "Robust lasing modes in coupled colloidal quantum dot microdisk pairs using a non-Hermitian exceptional point," Nat. Commun. **10**(1), 561 (2019).
64. Q. T. Cao, Y. L. Chen, and Y. F. Xiao, "Chiral emission and Purcell enhancement in a hybrid plasmonic-photonic microresonator," Light: Sci. Appl. **9**(1), 4 (2020).
65. T. Wu, W. X. Zhang, H. Z. Zhang, S. S. Hou, G. Y. Chen, R. B. Liu, C. C. Lu, J. F. Li, R. Y. Wang, P. F. Duan, J. J. Li, B. Wang, L. Shi, J. Zi, and X. D. Zhang, "Vector exceptional points with strong superchiral fields," Phys. Rev. Lett. **124**(8), 083901 (2020).
66. Y. Lumer, Y. Plotnik, M. C. Rechtsman, and M. Segev, "Nonlinearly induced PT transition in photonic systems," Phys. Rev. Lett. **111**(26), 263901 (2013).
67. A. U. Hassan, H. Hodaei, M.-A. Miri, M. Khajavikhan, and D. N. Christodoulides, "Nonlinear reversal of the $\mathcal{PT}$-symmetric phase transition in a system of coupled semiconductor microring resonators," Phys. Rev. A **92**(6), 063807 (2015).
68. M.-A. Miri and A. Alù, "Nonlinearity-induced pt-symmetry without material gain," New J. Phys. **18**(6), 065001 (2016).
69. Y.-X. Wang and A. A. Clerk, "Non-Hermitian dynamics without dissipation in quantum systems," Phys. Rev. A **99**(6), 063834 (2019).
70. A. Roy, S. Jahani, Q. Guo, A. Dutt, S. Fan, M.-A. Miri, and A. Marandi, "Nondissipative non-Hermitian dynamics and exceptional points in coupled optical parametric oscillators," Optica **8**(3), 415–421 (2021).
71. J. Ma, J. Wen, S. Ding, S. Li, Y. Hu, X. Jiang, L. Jiang, and M. Xiao, "Chip-based optical isolator and nonreciprocal parity-time symmetry induced by stimulated Brillouin scattering," Laser Photonics Rev. **14**(5), 1900278 (2020).
72. N. S. Makarov, M. Drobizhev, and A. Rebane, "Two-photon absorption standards in the 550–1600 nm excitation wavelength range," Opt. Express **16**(6), 4029–4047 (2008).
73. H. You, S. M. Hendrickson, and J. D. Franson, "Analysis of enhanced two-photon absorption in tapered optical fibers," Phys. Rev. A **78**(5), 053803 (2008).
74. X. Dai, X. Zhang, I. M. Kislyakov, L. Wang, J. Huang, S. Zhang, N. Dong, and J. Wang, "Enhanced two-photon absorption and two-photon luminescence in monolayer MoS2 and WS2 by defect repairing," Opt. Express **27**(10), 13744–13753 (2019).
75. M. A. Miri and A. Alù, "Exceptional points in optics and photonics," Science **363**(6422), eaar7709 (2019).
76. S. K. Ozdemir, S. Rotter, F. Nori, and L. Yang, "Parity-time symmetry and exceptional points in photonics," Nat. Mater. **18**(8), 783–798 (2019).
77. A. Miranowicz, J. Bajer, M. Paprzycka, Y.-X. Liu, A. M. Zagoskin, and F. Nori, "State-dependent photon blockade via quantum-reservoir engineering," Phys. Rev. A **90**(3), 033831 (2014).
78. E. S. Guerra, B. M. Garraway, and P. L. Knight, "Two-photon parametric pumping versus two-photon absorption: A quantum jump approach," Phys. Rev. A **55**(5), 3842–3857 (1997).
79. Y. R. Shen, "Quantum statistics of nonlinear optics," Phys. Rev. **155**(3), 921–931 (1967).
80. T. K. Fryett, C. M. Dodson, and A. Majumdar, "Cavity enhanced nonlinear optics for few photon optical bistability," Opt. Express **23**(12), 16246–16255 (2015).
81. K. Xia, G. Lu, G. Lin, Y. Cheng, Y. Niu, S. Gong, and J. Twamley, "Reversible nonmagnetic single-photon isolation using unbalanced quantum coupling," Phys. Rev. A **90**(4), 043802 (2014).
82. K. Xia, F. Nori, and M. Xiao, "Cavity-free optical isolators and circulators using a chiral cross-Kerr nonlinearity," Phys. Rev. Lett. **121**(20), 203602 (2018).
83. Z. Shen, Y.-L. Zhang, Y. Chen, F.-W. Sun, X.-B. Zou, G.-C. Guo, C.-L. Zou, and C.-H. Dong, "Reconfigurable optomechanical circulator and directional amplifier," Nat. Commun. **9**(1), 1797 (2018).
84. S. Zhang, Y. Hu, G. Lin, Y. Niu, K. Xia, J. Gong, and S. Gong, "Thermal-motion-induced non-reciprocal quantum optical system," Nat. Photonics **12**(12), 744–748 (2018).
85. Z. Shen, Y.-L. Zhang, Y. Chen, C.-L. Zou, Y.-F. Xiao, X.-B. Zou, F.-W. Sun, G.-C. Guo, and C.-H. Dong, "Experimental realization of optomechanically induced non-reciprocity," Nat. Photonics **10**(10), 657–661 (2016).

Optics EXPRESS

86. L. Tang, J. Tang, W. Zhang, G. Lu, H. Zhang, Y. Zhang, K. Xia, and M. Xiao, "On-chip chiral single-photon interface: Isolation and unidirectional emission," Phys. Rev. A **99**(4), 043833 (2019).
87. S. Zhang, G. Lin, Y. Hu, Y. Qi, Y. Niu, and S. Gong, "Cavity-free circulator with low insertion loss using hot atoms," Phys. Rev. Appl. **14**(2), 024032 (2020).
88. C. Liang, B. Liu, A.-N. Xu, X. Wen, C. Lu, K. Xia, M. K. Tey, Y.-C. Liu, and L. You, "Collision-induced broadband optical nonreciprocity," Phys. Rev. Lett. **125**(12), 123901 (2020).
89. Y. Shi, Z. Yu, and S. Fan, "Limitations of nonlinear optical isolators due to dynamic reciprocity," Nat. Photonics **9**(6), 388–392 (2015).
90. L. D. Bino, J. M. Silver, M. T. M. Woodley, S. L. Stebbings, X. Zhao, and P. Del'Haye, "Microresonator isolators and circulators based on the intrinsic nonreciprocity of the kerr effect," Optica **5**(3), 279–282 (2018).
91. D. L. Sounas, J. Soric, and A. Alù, "Broadband passive isolators based on coupled nonlinear resonances," Nat. Electron. **1**(2), 113–119 (2018).
92. K. Y. Yang, J. Skarda, M. Cotrufo, A. Dutt, G. H. Ahn, M. Sawaby, D. Vercruysse, A. Arbabian, S. Fan, A. Alù, and J. Vučković, "Inverse-designed non-reciprocal pulse router for chip-based lidar," Nat. Photonics **14**(6), 369–374 (2020).
93. L. Tang, J. Tang, H. Wu, J. Zhang, M. Xiao, and K. Xia, "Broad-intensity-range optical nonreciprocity based on feedback-induced Kerr nonlinearity," *Photon. Res.*, in press (2021).